
De novo antibody design with SE(3) diffusion

Daniel Cutting^{1*} Frédéric A. Dreyer^{1*} David Errington¹ Constantin Schneider¹
Charlotte M. Deane^{1,2}

¹Exscientia, Oxford Science Park, Oxford, OX4 4GE, UK

²Department of Statistics, University of Oxford, Oxford OX1 3LB, UK
{dcutting,fdreyer,derrington,cschneider}@exscientia.co.uk
deane@stats.ox.ac.uk

Abstract

We introduce *IgDiff*, an antibody variable domain diffusion model based on a general protein backbone diffusion framework which was extended to handle multiple chains. Assessing the designability and novelty of the structures generated with our model, we find that *IgDiff* produces highly designable antibodies that can contain novel binding regions. The backbone dihedral angles of sampled structures show good agreement with a reference antibody distribution. We verify these designed antibodies experimentally and find that all express with high yield. Finally, we compare our model with a state-of-the-art generative backbone diffusion model on a range of antibody design tasks, such as the design of the complementarity determining regions or the pairing of a light chain to an existing heavy chain, and show improved properties and designability.

1 Introduction

Engineering novel proteins that can satisfy specified functional properties is the central aim of rational protein design. While sequence-based methods have seen some success [Wu et al., 2021], they are intrinsically limited by the fact that most properties of a molecule, such as binding or solubility, are determined by their three-dimensional structure. Recent advances in diffusion models [Ho et al., 2020, Song et al., 2021], a class of deep probabilistic generative models, have shown promise as a data-driven alternative to more computationally expensive physics-based methods [Alford et al., 2017] in tackling *de novo* protein design. Most approaches focus on modelling only the backbone [Watson et al., 2022, Lin and AlQuraishi, 2023], while the sequence is inferred through an inverse folding model, though some full-atom models have been explored [Chu et al., 2023, Martinkus et al., 2023].

An application of particular therapeutic relevance is the design of immunoglobulin proteins, which play a central role in helping the adaptive immune system identify and neutralise pathogens. They consist of two heavy and two light chains. These are separated into constant domains that specify effector function, and a variable domain that contains six hypervariable loops, known as the complementarity determining regions (CDRs), which control binding specificity. The third loop of the heavy chain, CDR-H3, is the most structurally diverse domain of the antibody, and often determines antigen recognition [Narciso et al., 2011, Tsuchiya and Mizuguchi, 2016]. Monoclonal antibodies are an emerging drug modality with the potential for applications in a wide range of therapeutic areas, for example oncogenic, infectious and autoimmune diseases. They can be adapted to target specific antigens or receptors through engineering of the binding site [Chiu et al., 2019].

In this article, we consider the recent backbone diffusion model *FrameDiff* [Yim et al., 2023] and adapt it for applications to antibody variable regions. We then fine-tune it on synthetic antibody structures from the ImmuneBuilder dataset [Abanades et al., 2022]. Our *IgDiff* model is trained

*Equal contribution.

to generate the paired variable region backbone, with a paired heavy and light chain. We study the designability and novelty of the structures generated by our heavy chain model and predict the corresponding sequences with AbMPNN [Dreyer et al., 2023], an antibody-specific inverse folding model based on ProteinMPNN [Dauparas et al., 2022]. We then consider a range of design tasks and show how *IgDiff* can outperform existing backbone diffusion methods on antibody engineering tasks.

2 Related work

Denosing diffusion probabilistic models [Sohl-Dickstein et al., 2015, Ho et al., 2020] have shown promising results to the task of *de novo* protein design. Recent models based on a C_α -only backbone representation of proteins [Trippe et al., 2023] have already been adapted to account for the full frame representation of backbone residues [Yim et al., 2023, Lin and AlQuraishi, 2023] through the application of diffusion on Riemannian manifolds [Bortoli et al., 2022]. Notably, tools such as RFDiffusion [Watson et al., 2022], which rely on a fine-tuned RoseTTAFold structure prediction network for the reverse diffusion process, can tackle a number of complex protein engineering tasks such as protein binder design, enzyme active site scaffolding or topology-constrained protein monomer design. These diffusion models often operate in structural space, and an inverse folding model such as ProteinMPNN [Ingraham et al., 2019, Dauparas et al., 2022] is needed to recover sequences corresponding to the predicted structures. To reconstruct the placement of side-chain atoms, physics-based methods packing tools such as Rosetta [Alford et al., 2017] can be used. AI-driven side-chain packing methods based on SE(3) transformers [Fuchs et al., 2020], or a diffusion model on the joint distribution of torsional angles [Zhan et al., 2023] can also offer an efficient alternative.

Alternatively, protein diffusion models have been applied in sequence space to directly generate amino acid sequences [Lisanza et al., 2023] which can allow for sequence specific attributes and functional properties. Classifier-guided discrete diffusion models such as NOS [Gruver et al., 2023] can for example leverage a discriminative model and the large amount of available sequence data to predict sequences with high fitness.

Antibody design has seen rapid progress and will benefit from these advances in generative protein models. This task was traditionally tackled using energy-based optimization strategies [Li et al., 2014, Adolf-Bryfogle et al., 2018], and more recently with sequence-based language models [Liu et al., 2019, Saka et al., 2021]. Several structure-based approaches relying on graph neural networks, such as RefineGNN [Jin et al., 2022b], HSRN [Jin et al., 2022a], MEAN [Kong et al., 2023b] and its subsequent end-to-end design model dyMEAN [Kong et al., 2023a], or sequence and structure co-design diffusion models Luo et al. [2022], have shown promising results in predicting the CDR design of antibodies to target a specific epitope on an antigen. The *FrameDiff* framework has also been recently explored for inpainting CDR loops of T-cell receptors [Zhang et al., 2023], while other recent work has explored the application of structure-based diffusion models to the design of nanobodies [Bennett et al., 2024] and antibodies [Martinkus et al., 2023].

3 SE(3) protein backbone diffusion model

We review the SE(3) diffusion framework introduced by Yim et al. [2023], which constructs an explicit framework for the diffusion of protein backbones based on the Riemannian score-based generative modeling approach of Bortoli et al. [2022].

For the backbone frame parametrisation we adopt the same formalism as in AlphaFold2 [Jumper et al., 2021], using a collection of N orientation preserving rigid transformations to represent an N residue backbone, as shown in figure 1. These frames map from fixed coordinates of the four heavy atoms $N^*, C_\alpha^*, C^*, O^* \in \mathbb{R}^3$ centered at $C_\alpha^* = \vec{0}$, assuming experimentally measured bond lengths and angles [Engl and Huber, 2012]. The main backbone atomic coordinates for a residue i are given through

$$[N_i, C_i, C_{\alpha,i}] = T_i \cdot [N^*, C^*, C_\alpha^*], \quad (1)$$

where $T_i \in \text{SE}(3)$ is a member of the special Euclidean group, the set of valid translations and rotations in Euclidean space. A backbone consists of N frames $[T_1, \dots, T_N] \in \text{SE}(3)^N$, with the oxygen atom O being reconstructed from an additional torsion angle $\psi \in \text{SO}(2)$ around the C_α and C bond. Each frame is decomposed into $T_i = (r_i, x_i)$, where $x_i \in \mathbb{R}^3$ is the C_α translation and $r_i \in \text{SO}(3)$ is a 3×3 rotation matrix which can be derived from relative atom positions with the

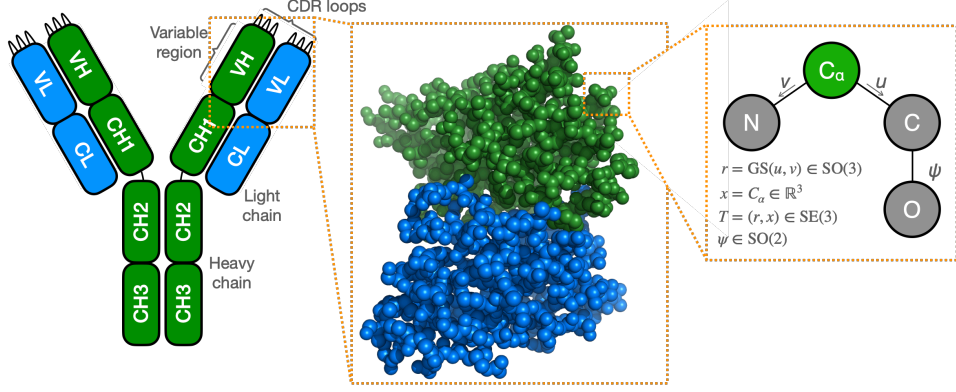


Figure 1: Left: Schematic representation of an antibody. Centre: Backbone atoms of the variable region, showing both a heavy (green) and light (blue) chain domain. Right: The parametrisation of residues into frames used by the diffusion model, with each frame consisting of four heavy atoms connected by rigid covalent bonds.

Gram-Schmidt process. A diffusion process over $SE(3)^N$ can be constructed to achieve global $SE(3)$ invariance by keeping the diffusion process centered at the origin.

We model the distribution over $SE(3)^N$ through Riemannian score-based generative modeling, which aims to sample from a distribution supported on a Riemannian manifold \mathcal{M} by reversing a forward process that evolves from the data distribution p_0 towards an invariant density p_T through

$$d\mathbf{X}_t = -\frac{1}{2}\nabla U(\mathbf{X}_t)dt + d\mathbf{B}_{t,\mathcal{M}}, \quad \mathbf{X}_0 \sim p_0, \quad (2)$$

where $\mathbf{B}_{t,\mathcal{M}}$ is the Brownian motion on \mathcal{M} , $U(x)$ is a continuously differentiable variable defining the invariant density $p_T \propto e^{-U(x)}$, ∇ is the Riemannian gradient, and $t \in [0, T]$ is a continuous time variable. The time-reversed process for $\mathbf{Y}_t = \mathbf{X}_{T-t}$ also satisfies a stochastic differential equation given by

$$d\mathbf{Y}_t = \left[\frac{1}{2}\nabla U(\mathbf{Y}_t) + \nabla \log p_{T-t}(\mathbf{Y}_t)\right]dt + d\mathbf{B}_{t,\mathcal{M}}, \quad \mathbf{Y}_0 \sim p_T, \quad (3)$$

where p_t is the density of \mathbf{X}_t . The Riemannian gradients and Brownian motion depend on a choice of inner product on \mathcal{M} , which for $SE(3)$ can simply be derived from the canonical inner products on $SO(3)$ and \mathbb{R}^3 . The invariant density on $SE(3)$ is chosen as $p_T \propto \mathcal{U}^{SO(3)}(r)\mathcal{N}(x)$.

The Stein score $\nabla \log p_t$ itself is intractable and is therefore approximated with a score network s_θ which is trained with a denoising score matching loss given by

$$\mathcal{L}_{\text{DSM}}(\theta) = \mathbb{E}[\lambda_t \|\nabla \log p_{t|0}(\mathbf{X}_t | \mathbf{X}_0) - s_\theta(t, \mathbf{X}_t)\|^2], \quad (4)$$

where λ_t is a weighting schedule, $p_{t|0}$ is the density of \mathbf{X}_t given \mathbf{X}_0 , and the expectation is taken over t and the distribution of $(\mathbf{X}_0, \mathbf{X}_t)$. The loss on $SE(3)$ is decomposed into its translation and rotation components as $\mathcal{L}_{\text{DSM}} = \mathcal{L}_{\text{DSM}}^x + \mathcal{L}_{\text{DSM}}^r$.

To mitigate chain breaks or steric clashes and to learn the torsion angle ψ , two auxiliary losses are used. The first one is a direct mean squared error on the backbone positions \mathcal{L}_{bb} , while the second one is a local neighbourhood loss on pairwise atomic distances \mathcal{L}_{2D} . These losses are applied with a weight w when sampling t near 0, when fine-grained characteristics of the protein backbone emerge, such that the full training loss is expressed as

$$\mathcal{L} = \mathcal{L}_{\text{DSM}} + w \Theta\left(\frac{T}{4} - t\right)(\mathcal{L}_{bb} + \mathcal{L}_{2D}). \quad (5)$$

The score network is based on the structure module of AlphaFold2 [Jumper et al., 2021] and performs iterative updates over L layers by combining spatial and sequence based attention modules using an Invariant Point Attention and a Transformer [Vaswani et al., 2017], considering a fully connected graph structure. As well as a denoised frame, the network also predicts the torsion angle ψ for each residue, from which the positions of the backbone oxygen atoms can be reconstructed.

Sampling is achieved through an Euler-Maruyama discretisation of equation (3) which is approximated with a geodesic random walk [Jørgensen, 1975]. To avoid destabilisation of the backbone

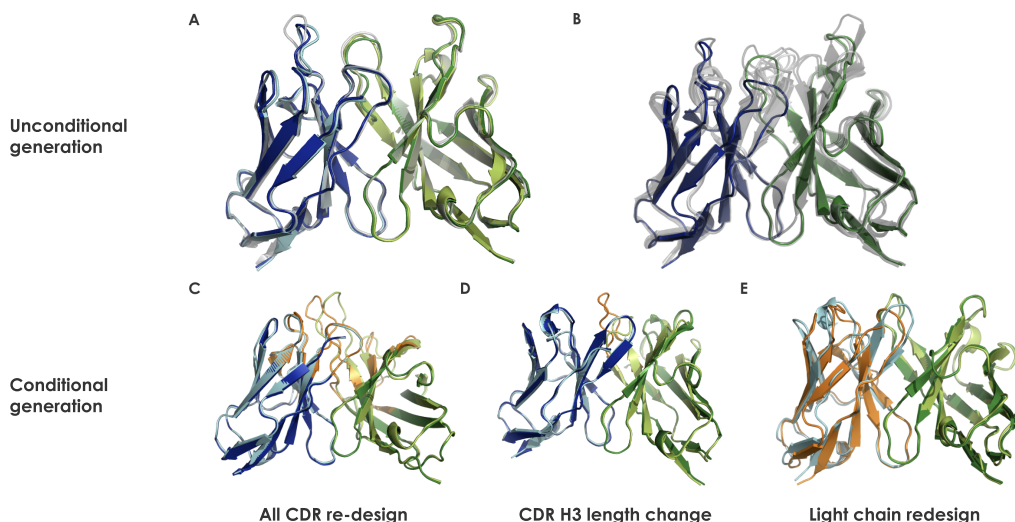


Figure 2: Examples of *IgDiff* generated antibody structures. Light chains are highlighted in blue, heavy chains in green. **(A-B)** Unconditionally generated antibodies. **(A)** *IgDiff* generated antibody (dark green/dark blue) compared to ABodyBuilder2 prediction on the lowest self-consistency RMSD sequence predicted by AbMPNN (light green/cyan) and the closest match in the training set by TM-score (grey). **(B)** Multiple antibodies generated by *IgDiff* with the same heavy and light chain length settings. **(C-E)** Conditionally generated antibodies, designed regions in orange, non-designed regions in dark blue/dark green, original input structure in cyan/light green. **(C)** Conditional generation of all CDR loops. **(D)** Conditional generation of CDR H3 with a different length compared to the input structure. **(E)** Conditional generation of the entire light chain.

in the final sampling steps, trajectories are instead truncated at a time $\epsilon > 0$. For all numerical applications, we use identical parameters to the original *FrameDiff* model [Yim et al., 2023].

We train this SE(3) diffusion model on synthetic antibody structural data, specifically targeting the variable domains whose CDR loops play a key role in defining the binding properties of the antibody. Our dataset consists of 148,832 variable regions from the Observed Antibody Space (OAS) [Kovaltsuk et al., 2018, Olsen et al., 2022], a database of antibody sequences, for which structures were predicted with ABodyBuilder2 (ABB2) [Abanades et al., 2022], an antibody structure prediction model based on the structure module of AlphaFold-Multimer [Evans et al., 2022].

Our *IgDiff* model is obtained by fine-tuning the updated *FrameDiff* weights from July 2023 for 18 hours on 8 NVIDIA A10G GPUs, using an Adam optimizer [Kingma and Ba, 2017] with a learning rate of 10^{-4} and a batch size of 64. To encode the chain break between the heavy and light domains, we add a jump of 50 in the residue index across chains. We also include a heavy or light chain label as an additional node feature. The training data is obtained by clustering the concatenated CDR heavy and light chain sequences at 80% similarity using CDHIT [Fu et al., 2012]. For each epoch, we train on one representative from each cluster. Batches are constructed from equal length antibodies, where we complete a batch with previously seen antibodies if necessary.

In Figure 2, we show examples of unconditioned structures obtained with *IgDiff*, as well as conditioned samples for each of the design tasks considered in this study. In order to determine the CDR regions, we use the IMGT numbering scheme [Lefranc et al., 2003] and North definition [North et al., 2011] throughout our analysis.

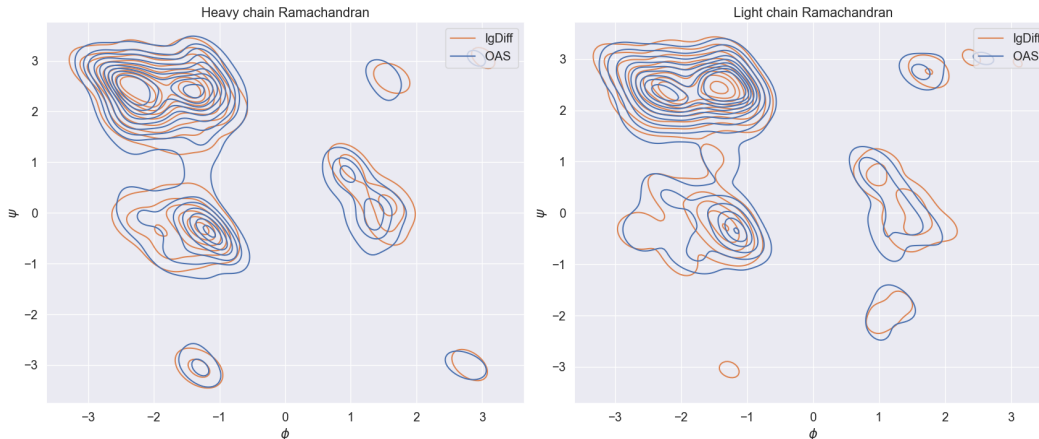


Figure 3: Left: Ramachandran plot of the dihedral angle distribution comparing the heavy chain residues from the predicted structures of OAS to *IgDiff*. Right: Same comparison for the light chain.

4 Generating *de novo* antibody variable domains

Let us now consider samples generated with *IgDiff* and study their properties. We first analyse the ability of our *IgDiff* model to sample plausible, novel, and diverse antibodies, when generating the entire variable domain backbone of both heavy and light chains.

Using our fine-tuned model, we start by sampling unconditioned paired heavy and light variable region structures. We obtain 100 unique combinations of chain lengths by sampling uniformly for the heavy and light chain independently between the 2.5 and 97.5 percentiles of the corresponding lengths found in the paired OAS. We then sample 8 structures for each of the 100 unique combinations for a total of 800 unique structures generated with *IgDiff*.

Sequences are predicted using the antibody-specific inverse folding model AbMPNN [Dreyer et al., 2023], an adaptation of the general protein model ProteinMPNN [Dauparas et al., 2022] to antibodies. We sample 20 sequences for each generated structure with temperature $T = 0.2$. To determine the best sequence for a given structure, we fold the sequence with ABB2 and compare it to the *IgDiff* structure. The root mean squared deviation (RMSD) between the model predicted for a sequence and the initial generated structure is referred to as the self-consistency RMSD (scRMSD). For each generated sample, we keep the sequence that results in the lowest scRMSD.

For consistency and diversity metrics, we compare to a baseline of 800 structures drawn from the training set of ABB2 predictions on paired OAS. For a fair comparison, we select 8 structures for each unique length combination of light and heavy chains in the *IgDiff* unconditioned dataset.

4.1 Consistency

We demonstrate that the *IgDiff* generated structures follow consistent structural distributions by comparing their backbone dihedral angle distributions in Ramachandran space to that of the OAS dataset. In Fig. 3, we show that the *IgDiff* ϕ and ψ angle distribution closely matches that of the structures of naturally occurring antibody sequences from the paired OAS predicted with the modelling tool ABB2.

All generated antibodies have an scRMSD for the best predicted sequence that is below 2\AA across the entire antibody, while 88% pass this threshold across each region independently, including all CDR loops. We also assess the consistency by considering the canonical clusters assumed by the CDR loops [Chothia and Lesk, 1987] and comparing those with the repredicted ABB2 structures, finding that across each region, more than 91% are assigned to the same canonical form. Further studies of the scRMSD of generated antibodies and the distribution of canonical clusters in the CDR loops are given in Appendix A.

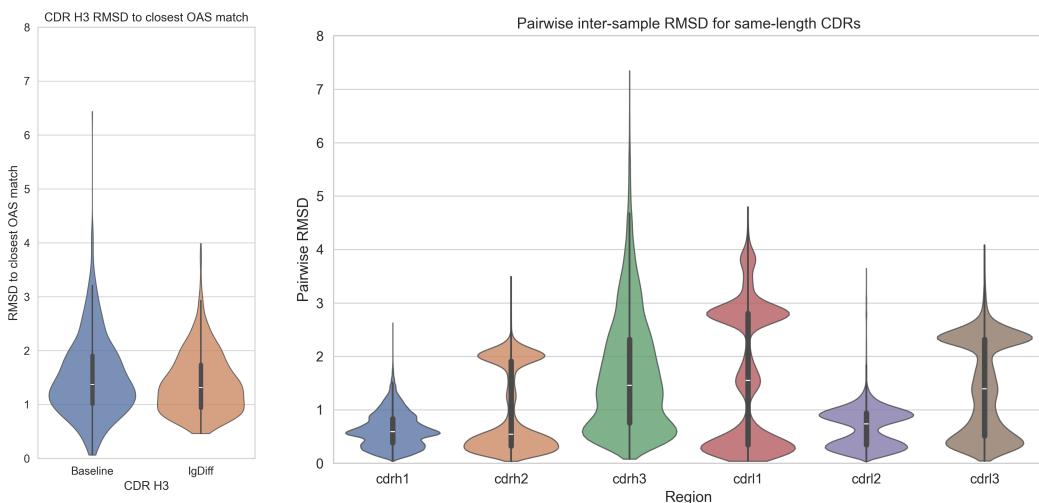


Figure 4: Left: Novelty of generated CDR H3 structures compared to random samples from the OAS dataset. For each structure, the RMSD shown is the CDR H3 RMSD to the closest match in the OAS dataset by TM-score with the same CDR H3 length. Right: Pairwise RMSD between *IgDiff* generated CDR loops of the same length.

When ABB2 outputs a prediction of a structure from a sequence, it first predicts an ensemble of four structures, and then selects the structure closest to the mean structure. This also allows it to provide a predicted error metric for each residue, computed from the mean deviation of the predicted residue position across the ensemble. When averaged across a set of residues this metric is referred to as the root mean square predicted error or RMSPE. We use the RMSPE evaluated across the full variable domain as an additional check for consistency, for which a generated structure will pass if the RMSPE is less than the 90th percentile of the RMSPE on the ABB2 testset. We find that 79.1% of our generated structures pass this test.

4.2 Novelty and diversity

We investigate the novelty of antibodies generated by *IgDiff* without conditioning by calculating the CDR H3 RMSD to the closest match by TM-score [Zhang and Skolnick, 2004] with identical CDR H3 loop length in the training dataset. This is shown in Fig. 4 (left), comparing the distribution of CDR H3 RMSD of *IgDiff* generated antibodies to that of a randomly drawn set of antibodies from the training dataset with the same distribution of CDR H3 loop lengths. Generated antibodies have similar novelty as randomly drawn antibodies from the training dataset, with mean CDR H3 RMSD to the closest match of $1.39\text{\AA} \pm 0.56$ for *IgDiff* generated antibodies and $1.50\text{\AA} \pm 0.74$ for naturally observed antibodies, demonstrating that the model can produce novel H3 loops.

We consider also the diversity of antibodies generated by *IgDiff*, an important consideration for antibody engineering. Taking CDRs with the same loop length, regardless of specified chain length, we calculate the pairwise RMSD between loops. This is shown in Fig. 4 (right), where we can observe diversity of generated CDR loops across different samples. Interestingly, we observe a bimodal distribution of pairwise RMSDs for CDRs L1, L3 and H2, arising from two generated loops either assuming the same or different canonical conformations. Further studies of the distribution of loop lengths as a function of specified chain length and exploration of sequence diversity are discussed in Appendix A.

4.3 Experimental validation

In order to demonstrate that *IgDiff* generated antibodies are able to express and exhibit favorable designability characteristics, we selected 28 antibody sequences for experimental validation. Prior to selection we first excluded any of the sequences that had higher than the median CDRH3 scRMSD or

Task	<i>IgDiff</i>			RFDiffusion		
	scRMSD	Confidence	Combined	scRMSD	Confidence	Combined
Unconditioned	0.88	0.79	0.76	-	-	-
Design all CDRs	0.04	0.80	0.02	0.00	0.54	0.00
Change CDRH3 length	0.76	0.91	0.74	0.08	0.69	0.06
Design light chain	0.93	1	0.93	-	-	-

Table 1: Success rate of inpainted samples for each design task and three different tests, comparing *IgDiff* and RFDiffusion. The scRMSD test requires all regions to have scRMSD $< 2\text{\AA}$ independently. The confidence test requires the ABB2 RMSPE averaged over all residues to be less than the 90th percentile of the same metric evaluated on the ABB2 test set. The combined test metric reports the fraction of designs passing both previous tests.

higher than the median overall scRMSD. As detailed in Appendix B all selected antibodies expressed and yielded sufficiently high concentration for downstream characterisation.

5 Antibody design tasks

Targeted design of specific regions of an antibody is of interest in a number of important applications. The engineering of the interface region, notably the CDR loops, can be of particular relevance for therapeutic applications [Akbar et al., 2021, Shanehsazzadeh et al., 2023]. Furthermore, the pairing of an appropriate heavy or light chain to a given domain is of importance in antibody discovery and in shaping antibody repertoires [DeKosky et al., 2015].

We thus consider the performance of *IgDiff* on conditional sampling for several inpainting design tasks of particular relevance to antibody engineering. The tasks we consider are (i) the design of all CDR loops given a fixed heavy and light chain framework, (ii) the design of a complete light chain given a heavy chain, and (iii) the design of a CDRH3 loop with varying length given the remaining variable region, thus allowing for additional contact interactions from the longer loop.

We generate 10 structures per reference structure and CDR length. All starting point antibodies are taken from the ABB2 test set. In order to perform inpainting, at each time t during inference we replace each frame in the fixed region with the corresponding frame from the reference structure after applying the forward noising process to time t .

In table 1, we show self-consistency metrics and compare our *IgDiff* model against RFDiffusion on each design task. None of the light chains designed by RFDiffusion can be parsed by Anarci [Dunbar and Deane, 2015] after inverse folding, while *IgDiff* always generates valid light chains, of which 93.3% pass our confidence and scRMSD test. The CDRH3 length change task leads to 74% of *IgDiff* generated structures that pass our combined test, compared with only 6% of RFDiffusion designs. For the task of designing all CDR loops, none of the RFDiffusion structures pass the scRMSD test, while 4% of the *IgDiff* structures have scRMSD below 2\AA across all regions. Note here that this low success rate in the case of *IgDiff* is primarily driven by a high scRMSD in the CDRH1 loop, while the remaining regions have a success rate above 75%. In contrast RFDiffusion also has poor self-consistency in CDRH1, CDRH3, CDRL1, and CDRL3. Further analysis of the scRMSD distribution and canonical clusters of designs, as well as details of the starting point antibodies used for each design task, are given in Appendix B.

6 Conclusions

In this article, we introduce a model for *de novo* antibody generation, *IgDiff*. This model is derived from the recent SE(3) diffusion framework *FrameDiff*, by fine-tuning on antibody variable domains. The weights of our *IgDiff* model are made publicly available [Dreyer and Cutting, 2024].

We show that our antibody backbone model is able to recapitulate the expected backbone dihedral distribution, and studied the validity of the sequences recovered from generated samples using an antibody-specific inverse folding model. Studying the designability of the generated structures by comparing them with structure predictions based on the corresponding sequences, we found excellent

agreement. We probed our model for novelty by finding the closest match in the training data for each sampled structure and found it could generate structures distinct from those in the training set. We selected a number of designs for experimental validation, finding that all generated antibodies express with high yield. We further found that *IgDiff* generates diverse antibodies, particularly in the CDR loops that are important determinants of binding affinity, making it well suited for antibody design tasks.

Finally, we considered examples of antibody engineering tasks, such as the redesign of CDR loops or the generation of a light chain paired to a specified heavy chain, and demonstrated the applicability of our approach in practical use cases. We designed metrics to assess the quality of generated structures, and showed substantial improvement over existing state-of-the-art protein diffusion models.

Diffusion models trained on antibodies offer a promising approach to accelerate drug design through data-driven generative AI. In this article, we provide a key step towards the generation of viable therapeutic antibodies through structure-based diffusion. Conditioning the generation of samples to express desired properties, as well as to target specified antigens, will be a crucial elements towards facilitating their application in therapeutic development.

Acknowledgements

We are grateful to Henry Kenlay, Claire Marks, Douglas Pires, Aleksandr Kovaltsuk and Newton Wahome for useful discussions.

A Designability and novelty of unconditioned generation

In Figure 5, we show the expression yields for 28 selected antibody sequences predicted with AbMPNN from full unconditioned variable structures produced with *IgDiff*.



Figure 5: Expression yields (mg/L) of a validation set of *IgDiff* generated antibodies.

We assess the scRMSD of *IgDiff* generated antibody structures to corresponding ABB2 predicted structures. To this end, we predict 20 amino acid sequences for each *IgDiff* generated backbone structure using AbMPNN and use ABB2 to predict the structure those sequences are likely to assume, reporting the scRMSDs for the AbMPNN prediction that achieves the lowest overall scRMSD across the 20 predictions for each *IgDiff* output, as shown in Fig. 6. A lower scRMSD in this scenario indicates that the *IgDiff* generated antibody structures represent realistic and designable antibody structures. We show that the structures are designable in that the scRMSD in all loops are typically lower than the 2 Å cutoff used to define designability in the original *FrameDiff* paper [Yim et al., 2023]. All *IgDiff* generated antibodies pass the 2Å threshold across the entire antibody and 88% of *IgDiff* generated antibodies also pass for every sub-region assessed independently in Fig. 6, including all CDR loops.

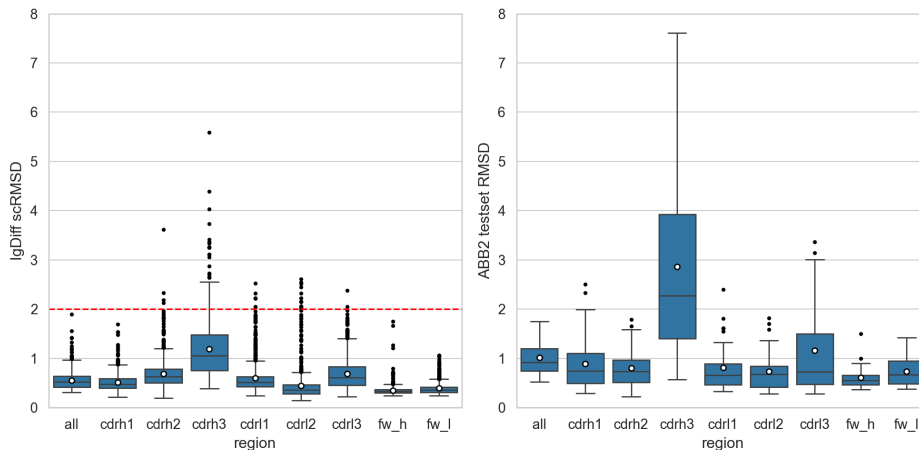


Figure 6: scRMSD of *IgDiff* structures against ABB2 re-predictions, compared to inherent ABB2 RMSD. **(Left)** *IgDiff* scRMSD to the ABB2 predicted structure for the AbMPNN sequence producing the lowest overall scRMSD to the input *IgDiff* structure. The red line indicates the 2Å cutoff used to designate a designable structure in *FrameDiff* [Yim et al., 2023]. **(Right)** RMSD of ABB2 predictions on the ABB2 testset against the ground truth crystal structures. Mean *IgDiff* scRMSD on each region are lower than the corresponding ABB2 test set RMSD.

Region	Matching clusters	Mismatching clusters	Both unclassified
CDRH1	0.98	0.01	0.01
CDRH2	0.92	0.00	0.08
CDRL1	0.93	0.03	0.04
CDRL2	0.95	0.01	0.04
CDRL3	0.85	0.09	0.06

Table 2: Canonical cluster analysis of antibody structures generated unconditionally using *IgDiff* and the ABB2 repredicted structures.

We further assessed self-consistency through the canonical clusters assumed by the non-H3 CDR loops in both *IgDiff* generated structures and ABB2 repredicted structures (generated as described for the scRMSD calculation). To this end, each loop is assigned to the closest PyIGClassify cluster centre by RMSD Adolf-Bryfogle et al. [2015]. If a loop has an unusual length with no clusters or has $\text{RMSD} > 1.5\text{\AA}$ to the closest cluster centre then it is denoted as unclassified.

For non-H3 loops, *IgDiff* structures and ABB2 repredicted structures were assigned the same canonical class in between 93% (CDR L1) and 98% (CDR H1) of samples for the less variable CDRs 1 and 2 and in 85% of samples for the more variable CDR L3. Up to 8% (CDRH2) of generated designs fell outside of the known canonical class for that loop both in the *IgDiff* generated structure and in the ABB2 repredicted structure (see Table 2). We further show the RMSD to the assigned cluster centre for each loop generated by *IgDiff* and ABB2 respectively, as well as for a baseline of OAS paired ABB2 predicted structures (see Fig. 7). We demonstrate that RMSD to the closest cluster centre depends heavily on the canonical class of the loop and that *IgDiff* generated antibodies follow a similar distribution of distances to the closest cluster centre as the ABB2 repredicted structures and a baseline set of OAS derived, ABB2 predicted structures.

For heavy or light chains generated with the same length specification, we investigate the distribution of loop length for each CDR, as CDRs with different lengths can necessarily be considered diverse. This is shown in Fig. 8. We observe that *IgDiff* generates diverse CDR loop lengths largely independent of the pre-specified chain length. For the light chain, diversity of CDR loop lengths increases with increasing chain length, while for the heavy chain, the diversity of generated CDR loops remains broadly constant across chain lengths (with the exception of CDR H1 at short chain lengths). We further observe that *IgDiff* drives chain length of the heavy chain primarily via CDR H3 length and light chain length via CDR L1 and L3 length, mirroring the natural distributions of CDR loop lengths.

To explore sequence diversity, we find the minimum pairwise Levenshtein distance (also known as edit distance) between the sequence of a generated *IgDiff* structure and the sequences in the rest of the generated structures. The resulting distribution of pairwise distances is shown in Fig. 9. Each generated antibody has at least 3 edits between the closest sequence, and at most 56 edits. The median number of edits to the closest sequence is 15. For a comparison we also show the minimum pairwise edit distances between 800 example predicted structures taken from the paired OAS dataset with the same chain lengths as the *IgDiff* unconditioned dataset. Both distributions are similar, with *IgDiff* producing fewer antibodies with very low and very high minimum edit distances and more antibodies with medium edit distances than the OAS baseline.

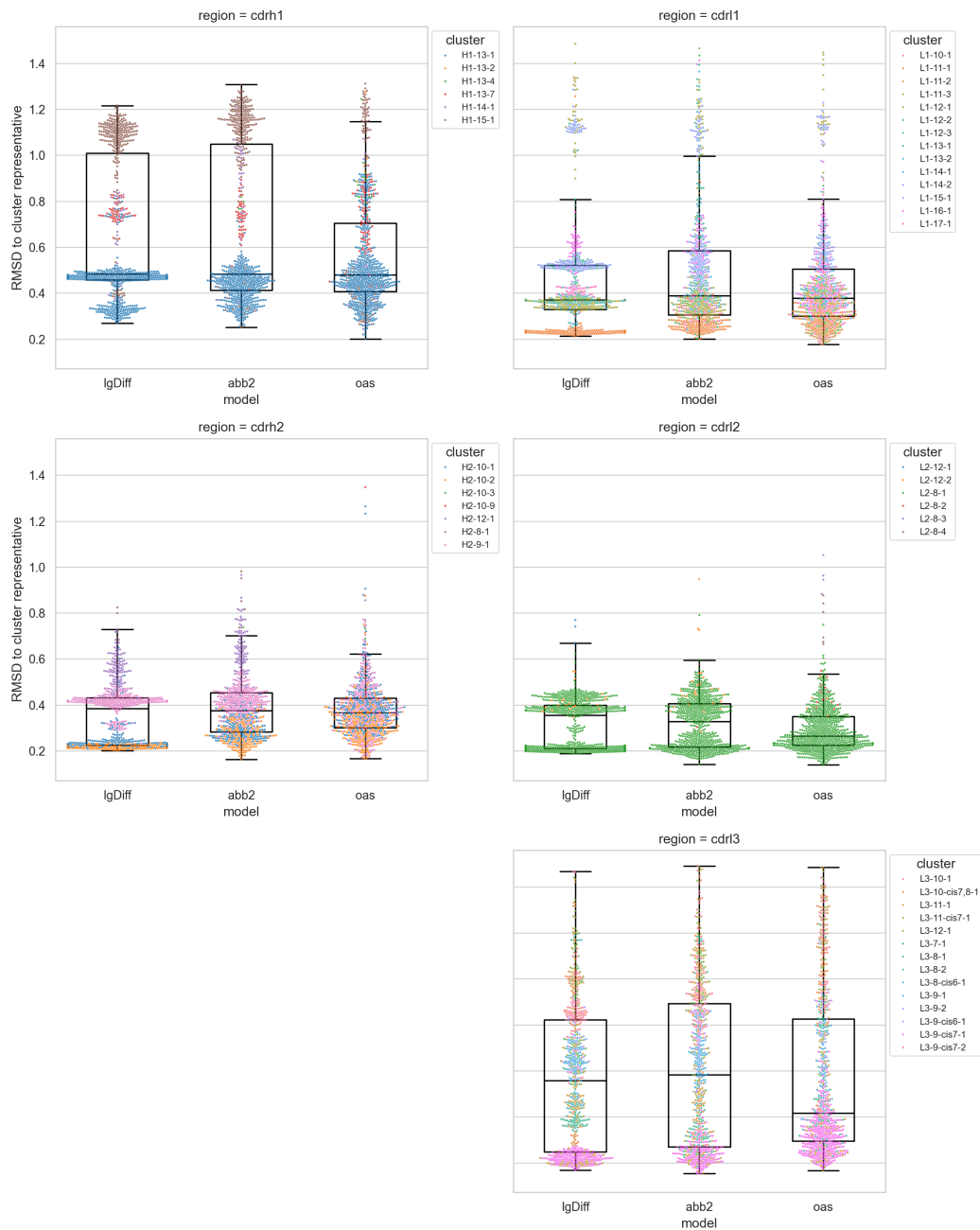


Figure 7: RMSD to the central cluster representative in the PyIGClassify dataset for all classified canonical loops. Each panel refers to a different CDR loop. For each panel we show the result for the generated *IgDiff* structures on the left, the results for the ABB2 structures predicted on the *IgDiff* sequences in the centre, and a baseline of paired OAS structure predictions on the right. In each plot the individual datapoints that make up a box-plot are shown as a swarm-plot with cluster class indicated by the point hue.

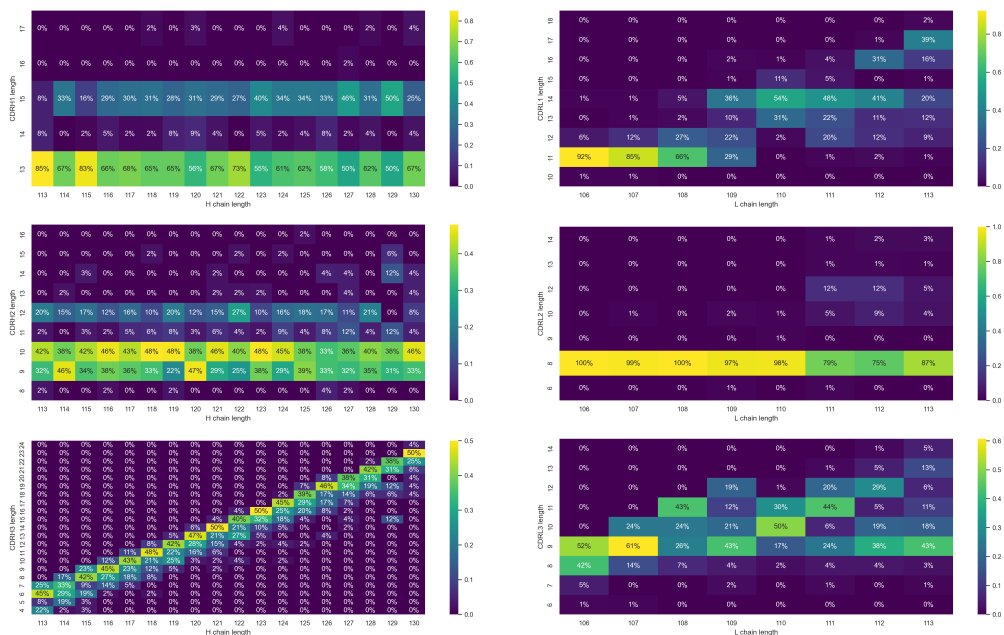


Figure 8: Distribution of CDR loop lengths depending on the generated heavy or light chain length.

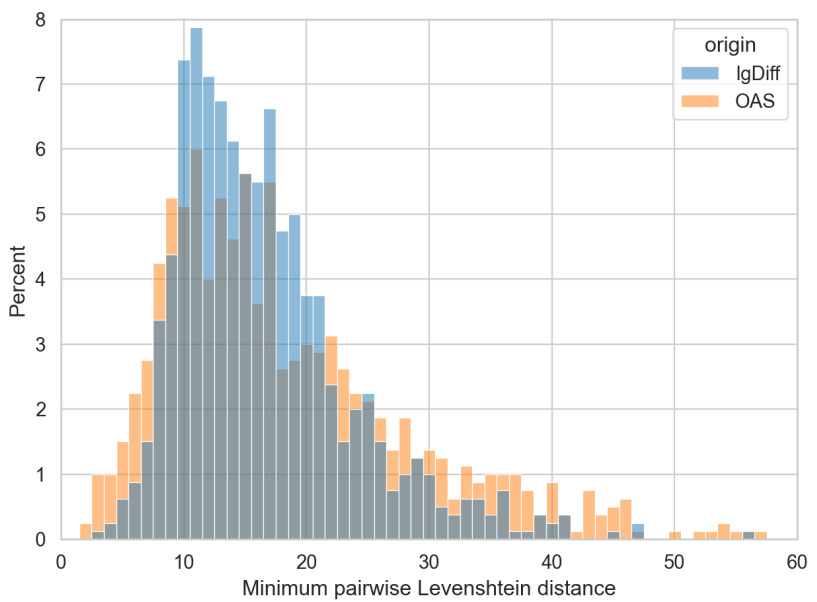


Figure 9: Histogram of the minimum pairwise Levenshtein distance between 800 unconditioned *IgDiff* generated structures (blue) and 800 paired OAS sequences (orange).

B Benchmarking of design tasks

The starting point antibodies used in each design task are given in Table 3. In this appendix, we consider also the task of redesigning the CDRL3 loop with varying lengths, to study the recapitulation of the canonical clusters of designs with modified loop lengths. This task is left out of the main text for conciseness but achieves 100% success on the scRMSD test for *IgDiff* compared to 85% for RFDiffusion, with both models obtaining 100% success on the confidence test.

Design task	Subtasks	Reference antibody	Total samples
CDRH3 length change	H3 lengths 10-19	7seg	100
CDRL3 length change	L3 lengths 8-11	7sem	40
Design all CDRs	Different antibodies	7ps6, 7q4q, 7rp2, 7ttm, 7u8c	50
Design light chain	Different heavy chains	7qf0, 7rxl, 7zf6	30

Table 3: Conditional design tasks. We sample 10 structures for each inpainting subtask. The CDRL3 length change design task is limited to this Appendix.

In Figure 10, we show the scRMSD of each region across the different design tasks. We compare the performance of *IgDiff* to the baseline of RFDiffusion. We see that in all design tasks *IgDiff* has a lower mean and median scRMSD in the region that is being inpainted. The most challenging task for *IgDiff* is to design all of the CDRs. Interestingly, the region that *IgDiff* most struggles to model in this conditional task appears to be CDRH1, although this region was well modelled in unconditional generation. For all other tasks, we show that almost all designed antibodies retain a scRMSD below 2Å across all regions, indicating that the conditioned antibodies retain the designability properties of the unconditioned model. Figure 11 shows the RMSD with the input structure across the fixed regions of the design task. This is below 1Å for all generated structures, demonstrating that the motifs are well preserved during the inpainting procedure.

In Table 4, we give the fraction of matching canonical clusters with repredicted ABB2 structures for each design task. Here we note good agreement across all CDR loops except CDR H1. Notably *IgDiff* outperforms RFDiffusion on the fraction of matching clusters on all tasks.

Task	Region	<i>IgDiff</i>			RFDiffusion		
		Matching clusters	Mismatching clusters	Both unclassified	Matching clusters	Mismatching clusters	Both unclassified
Design all CDRs	CDRH1	0.02	0.96	0.02	0.06	0.84	0.10
Design all CDRs	CDRH2	1.00	0.00	0.00	1.00	0.00	0.00
Design all CDRs	CDRL1	0.70	0.24	0.06	0.02	0.74	0.24
Design all CDRs	CDRL2	0.98	0.02	0.00	0.02	0.98	0.00
Design all CDRs	CDRL3	0.90	0.10	0.00	0.46	0.54	0.00
CDRL3 length change	CDRL3	0.70	0.28	0.03	0.68	0.33	0.00
Design light chain	CDRL1	0.80	0.17	0.03	–	–	–
Design light chain	CDRL2	1.00	0.00	0.00	–	–	–
Design light chain	CDRL3	0.87	0.07	0.07	–	–	–

Table 4: Fraction of matching and mismatching canonical clusters between the antibody structures generated conditionally using *IgDiff* and the ABB2 repredicted structures. Note that RFDiffusion did not produce antibody light chains in the light chain design task.

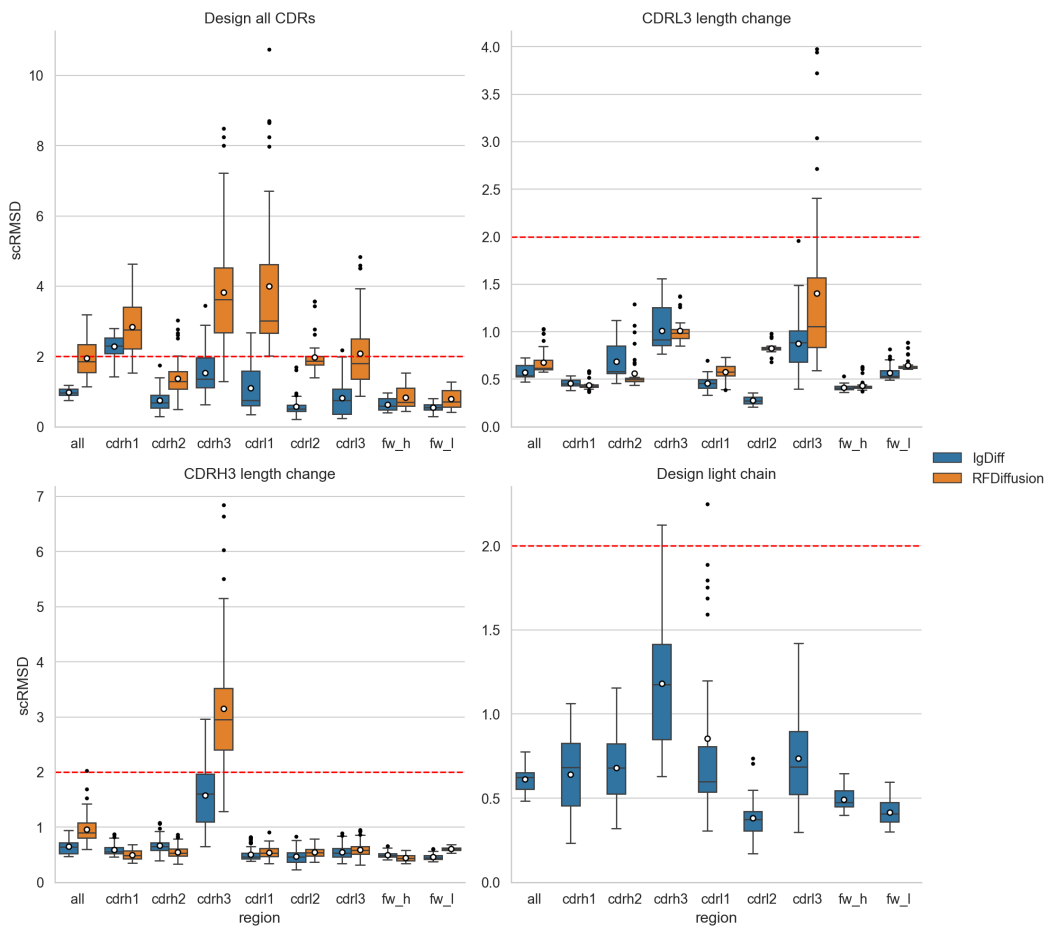


Figure 10: scRMSD of antibodies generated conditionally using *IgDiff* and RFDiffusion with different design tasks. The red line indicates the 2Å cutoff used to designate designable structures.

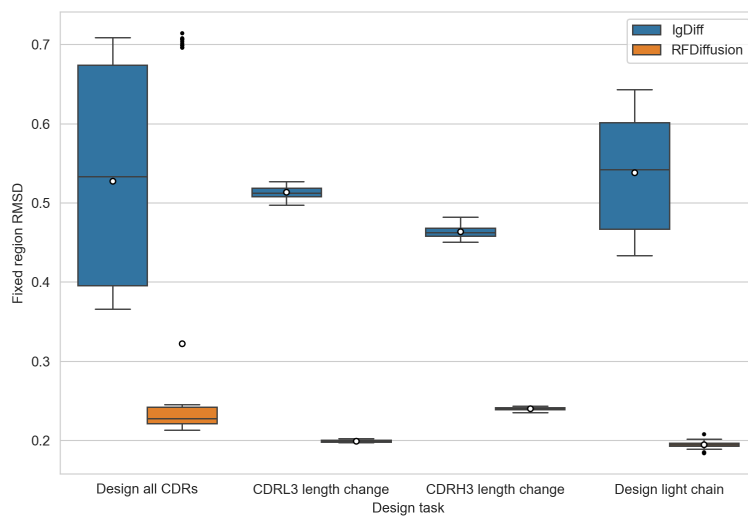


Figure 11: RMSD of the fixed regions during conditional design tasks using *IgDiff* and RFDiffusion. For each design task, the RMSD is evaluated on the fixed region and between the generated design and the reference antibody

References

- Brennan Abanades, Wing Ki Wong, Fergus Boyles, Guy Georges, Alexander Bujotzek, and Charlotte M. Deane. Immunebuilder: Deep-learning models for predicting the structures of immune proteins. *bioRxiv*, 2022. doi: 10.1101/2022.11.04.514231. URL <https://www.biorxiv.org/content/early/2022/11/04/2022.11.04.514231>.
- Jared Adolf-Bryfogle, Qifang Xu, Benjamin North, Andreas Lehmann, and Roland L Dunbrack Jr. Pyigclassify: a database of antibody cdr structural classifications. *Nucleic acids research*, 43(D1): D432–D438, 2015.
- Jared Adolf-Bryfogle, Oleks Kalyuzhniy, Michael Kubitz, Brian D. Weitzner, Xiaozhen Hu, Yumiko Adachi, William R. Schief, and Roland L. Dunbrack, Jr. Rosettaantibodydesign (rabd): A general framework for computational antibody design. *PLOS Computational Biology*, 14(4):1–38, 04 2018. doi: 10.1371/journal.pcbi.1006112. URL <https://doi.org/10.1371/journal.pcbi.1006112>.
- Rahmad Akbar, Philippe A. Robert, Milena Pavlović, Jeliasko R. Jeliaskov, Igor Snapkov, Andrei Slabodkin, Cédric R. Weber, Lonneke Scheffer, Enkelejda Miho, Ingrid Hobæk Haff, Dag Trygve Tryslew Haug, Fridtjof Lund-Johansen, Yana Safonova, Geir K. Sandve, and Victor Greiff. A compact vocabulary of paratope-epitope interactions enables predictability of antibody-antigen binding. *Cell Reports*, 34(11):108856, 2021. ISSN 2211-1247. doi: <https://doi.org/10.1016/j.celrep.2021.108856>. URL <https://www.sciencedirect.com/science/article/pii/S2211124721001704>.
- Rebecca F. Alford, Andrew Leaver-Fay, Jeliasko R. Jeliaskov, Matthew J. O’Meara, Frank P. DiMaio, Hahnbeom Park, Maxim V. Shapovalov, P. Douglas Renfrew, Vikram K. Mulligan, Kalli Kappel, Jason W. Labonte, Michael S. Pacella, Richard Bonneau, Philip Bradley, Roland L. Dunbrack, Rhiju Das, David Baker, Brian Kuhlman, Tanja Kortemme, and Jeffrey J. Gray. The rosetta all-atom energy function for macromolecular modeling and design. *Journal of Chemical Theory and Computation*, 13(6):3031–3048, June 2017. ISSN 1549-9618. doi: 10.1021/acs.jctc.7b00125.
- Nathaniel R. Bennett, Joseph L. Watson, Robert J. Ragotte, Andrew J. Borst, Déjenaé L. See, Connor Weidle, Riti Biswas, Ellen L. Shrock, Philip J. Y. Leung, Buwei Huang, Inna Goreschnik, Russell Ault, Kenneth D. Carr, Benedikt Singer, Cameron Criswell, Dionne Vafeados, Mariana Garcia Sanchez, Ho Min Kim, Susana Vázquez Torres, Sidney Chan, and David Baker. Atomically accurate de novo design of single-domain antibodies. *bioRxiv*, 2024. doi: 10.1101/2024.03.14.585103. URL <https://www.biorxiv.org/content/early/2024/03/18/2024.03.14.585103>.
- Valentin De Bortoli, Emile Mathieu, Michael Hutchinson, James Thornton, Yee Whye Teh, and Arnaud Doucet. Riemannian score-based generative modelling, 2022.
- Mark L Chiu, Dennis R Goulet, Alexey Teplyakov, and Gary L Gilliland. Antibody structure and function: the basis for engineering therapeutics. *Antibodies*, 8(4):55, 2019.
- Cyrus Chothia and Arthur M. Lesk. Canonical structures for the hypervariable regions of immunoglobulins. *Journal of Molecular Biology*, 196(4):901–917, 1987. ISSN 0022-2836. doi: [https://doi.org/10.1016/0022-2836\(87\)90412-8](https://doi.org/10.1016/0022-2836(87)90412-8). URL <https://www.sciencedirect.com/science/article/pii/0022283687904128>.
- Alexander E. Chu, Lucy Cheng, Gina El Nesr, Minkai Xu, and Po-Ssu Huang. An all-atom protein generative model. *bioRxiv*, 2023. doi: 10.1101/2023.05.24.542194. URL <https://www.biorxiv.org/content/early/2023/05/25/2023.05.24.542194>.
- J. Dauparas, I. Anishchenko, N. Bennett, H. Bai, R. J. Ragotte, L. F. Milles, B. I. M. Wicky, A. Courbet, R. J. de Haas, N. Bethel, P. J. Y. Leung, T. F. Huddy, S. Pellock, D. Tischer, F. Chan, B. Koepnick, H. Nguyen, A. Kang, B. Sankaran, A. K. Bera, N. P. King, and D. Baker. Robust deep learning based protein sequence design using proteinmpnn. *bioRxiv*, 2022. doi: 10.1101/2022.06.03.494563. URL <https://www.biorxiv.org/content/early/2022/06/04/2022.06.03.494563>.

- Brandon J DeKosky, Takaaki Kojima, Alexa Rodin, Wissam Charab, Gregory C Ippolito, Andrew D Ellington, and George Georgiou. In-depth determination and analysis of the human paired heavy- and light-chain antibody repertoire. *Nature Medicine*, 21(1):86–91, 2015. doi: 10.1038/nm.3743. URL <https://doi.org/10.1038/nm.3743>.
- Frédéric A. Dreyer, Daniel Cutting, Constantin Schneider, Henry Kenlay, and Charlotte M. Deane. Inverse folding for antibody sequence design using deep learning. In *2023 ICML Workshop on Computational Biology*, 2023. URL <https://arxiv.org/abs/2310.19513>.
- Frédéric A. Dreyer and Daniel Cutting. De novo antibody design with se(3) diffusion, May 2024. URL <https://doi.org/10.5281/zenodo.11184374>.
- James Dunbar and Charlotte M. Deane. ANARCI: antigen receptor numbering and receptor classification. *Bioinformatics*, 32(2):298–300, 09 2015. ISSN 1367-4803. doi: 10.1093/bioinformatics/btv552. URL <https://doi.org/10.1093/bioinformatics/btv552>.
- R. A. Engh and R. Huber. *Structure quality and target parameters*, chapter 18.3, pages 474–484. John Wiley & Sons, Ltd, 2012. ISBN 9780470685754. doi: <https://doi.org/10.1107/97809553602060000857>. URL <https://onlinelibrary.wiley.com/doi/abs/10.1107/97809553602060000857>.
- Richard Evans, Michael O’Neill, Alexander Pritzel, Natasha Antropova, Andrew Senior, Tim Green, Augustin Žídek, Russ Bates, Sam Blackwell, Jason Yim, Olaf Ronneberger, Sebastian Bodenstein, Michal Zielinski, Alex Bridgland, Anna Potapenko, Andrew Cowie, Kathryn Tunyasuvunakool, Rishub Jain, Ellen Clancy, Pushmeet Kohli, John Jumper, and Demis Hassabis. Protein complex prediction with alphafold-multimer. *bioRxiv*, 2022. doi: 10.1101/2021.10.04.463034. URL <https://www.biorxiv.org/content/early/2022/03/10/2021.10.04.463034>.
- Limin Fu, Beifang Niu, Zhengwei Zhu, Sitao Wu, and Weizhong Li. CD-HIT: accelerated for clustering the next-generation sequencing data. *Bioinformatics*, 28(23):3150–3152, 10 2012. ISSN 1367-4803. doi: 10.1093/bioinformatics/bts565. URL <https://doi.org/10.1093/bioinformatics/bts565>.
- Fabian B. Fuchs, Daniel E. Worrall, Volker Fischer, and Max Welling. Se(3)-transformers: 3d roto-translation equivariant attention networks. In *Advances in Neural Information Processing Systems 34 (NeurIPS)*, 2020.
- Nate Gruver, Samuel Stanton, Nathan C. Frey, Tim G. J. Rudner, Isidro Hotzel, Julien Lafrance-Vanasse, Arvind Rajpal, Kyunghyun Cho, and Andrew Gordon Wilson. Protein design with guided discrete diffusion, 2023.
- Jonathan Ho, Ajay Jain, and Pieter Abbeel. Denoising diffusion probabilistic models, 2020.
- John Ingraham, Vikas Garg, Regina Barzilay, and Tommi Jaakkola. Generative models for graph-based protein design. In H. Wallach, H. Larochelle, A. Beygelzimer, F. d’Alché-Buc, E. Fox, and R. Garnett, editors, *Advances in Neural Information Processing Systems*, volume 32. Curran Associates, Inc., 2019. URL https://proceedings.neurips.cc/paper_files/paper/2019/file/f3a4ff4839c56a5f460c88c3666a2b-Paper.pdf.
- Wengong Jin, Dr.Regina Barzilay, and Tommi Jaakkola. Antibody-antigen docking and design via hierarchical structure refinement. In Kamalika Chaudhuri, Stefanie Jegelka, Le Song, Csaba Szepesvari, Gang Niu, and Sivan Sabato, editors, *Proceedings of the 39th International Conference on Machine Learning*, volume 162 of *Proceedings of Machine Learning Research*, pages 10217–10227. PMLR, 17–23 Jul 2022a. URL <https://proceedings.mlr.press/v162/jin22a.html>.
- Wengong Jin, Jeremy Wohlwend, Regina Barzilay, and Tommi S. Jaakkola. Iterative refinement graph neural network for antibody sequence-structure co-design. In *International Conference on Learning Representations*, 2022b. URL https://openreview.net/forum?id=LI2bhrE_2A.
- Erik Jørgensen. The central limit problem for geodesic random walks. *Zeitschrift für Wahrscheinlichkeitstheorie und Verwandte Gebiete*, 32(1):1–64, 1975. doi: 10.1007/BF00533088. URL <https://doi.org/10.1007/BF00533088>.

- John Jumper, Richard Evans, Alexander Pritzel, Tim Green, Michael Figurnov, Olaf Ronneberger, Kathryn Tunyasuvunakool, Russ Bates, Augustin Žídek, Anna Potapenko, Alex Bridgland, Clemens Meyer, Simon A. A. Kohl, Andrew J. Ballard, Andrew Cowie, Bernardino Romera-Paredes, Stanislav Nikolov, Rishub Jain, Jonas Adler, Trevor Back, Stig Petersen, David Reiman, Ellen Clancy, Michal Zielinski, Martin Steinegger, Michalina Pacholska, Tamas Berghammer, Sebastian Bodenstein, David Silver, Oriol Vinyals, Andrew W. Senior, Koray Kavukcuoglu, Pushmeet Kohli, and Demis Hassabis. Highly accurate protein structure prediction with alphafold. *Nature*, 596(7873):583–589, 2021. doi: 10.1038/s41586-021-03819-2. URL <https://doi.org/10.1038/s41586-021-03819-2>.
- Diederik P. Kingma and Jimmy Ba. Adam: A method for stochastic optimization, 2017.
- Xiangzhe Kong, Wenbing Huang, and Yang Liu. End-to-end full-atom antibody design, 2023a.
- Xiangzhe Kong, Wenbing Huang, and Yang Liu. Conditional antibody design as 3d equivariant graph translation. In *The Eleventh International Conference on Learning Representations*, 2023b. URL <https://openreview.net/forum?id=LFHFQbjxIiP>.
- Aleksandr Kovaltsuk, Jinwoo Leem, Sebastian Kelm, James Snowden, Charlotte M. Deane, and Konrad Krawczyk. Observed Antibody Space: A Resource for Data Mining Next-Generation Sequencing of Antibody Repertoires. *The Journal of Immunology*, 201(8):2502–2509, 10 2018. ISSN 0022-1767. doi: 10.4049/jimmunol.1800708. URL <https://doi.org/10.4049/jimmunol.1800708>.
- Marie-Paule Lefranc, Christelle Pommié, Manuel Ruiz, Véronique Giudicelli, Elodie Foulquier, Lisa Truong, Valérie Thouvenin-Contet, and Gérard Lefranc. Imgt unique numbering for immunoglobulin and t cell receptor variable domains and ig superfamily v-like domains. *Developmental & Comparative Immunology*, 27(1):55–77, 2003. ISSN 0145-305X. doi: [https://doi.org/10.1016/S0145-305X\(02\)00039-3](https://doi.org/10.1016/S0145-305X(02)00039-3). URL <https://www.sciencedirect.com/science/article/pii/S0145305X02000393>.
- Tong Li, Robert J. Pantazes, and Costas D. Maranas. Optmaven – a new framework for the de novo design of antibody variable region models targeting specific antigen epitopes. *PLOS ONE*, 9(8):1–17, 08 2014. doi: 10.1371/journal.pone.0105954. URL <https://doi.org/10.1371/journal.pone.0105954>.
- Yeqing Lin and Mohammed AlQuraishi. Generating novel, designable, and diverse protein structures by equivariantly diffusing oriented residue clouds, 2023.
- Sidney Lyayuga Lianza, Jake Merle Gershon, Sam Tipps, Lucas Arnoldt, Samuel Hendel, Jeremiah Nelson Sims, Xinting Li, and David Baker. Joint generation of protein sequence and structure with rosettafold sequence space diffusion. *bioRxiv*, 2023. doi: 10.1101/2023.05.08.539766. URL <https://www.biorxiv.org/content/early/2023/05/10/2023.05.08.539766>.
- Ge Liu, Haoyang Zeng, Jonas Mueller, Brandon Carter, Ziheng Wang, Jonas Schilz, Geraldine Horny, Michael E Birnbaum, Stefan Ewert, and David K Gifford. Antibody complementarity determining region design using high-capacity machine learning. *Bioinformatics*, 36(7):2126–2133, 11 2019. ISSN 1367-4803. doi: 10.1093/bioinformatics/btz895. URL <https://doi.org/10.1093/bioinformatics/btz895>.
- Shitong Luo, Yufeng Su, Xingang Peng, Sheng Wang, Jian Peng, and Jianzhu Ma. Antigen-specific antibody design and optimization with diffusion-based generative models for protein structures. In Alice H. Oh, Alekh Agarwal, Danielle Belgrave, and Kyunghyun Cho, editors, *Advances in Neural Information Processing Systems*, 2022. URL <https://openreview.net/forum?id=jSorGn2Tjg>.
- Karolis Martinkus, Jan Ludwiczak, Kyunghyun Cho, Wei-Ching Liang, Julien Lafrance-Vanasse, Isidro Hotzel, Arvind Rajpal, Yan Wu, Richard Bonneau, Vladimir Gligorijevic, and Andreas Loukas. Abdiffuser: Full-atom generation of in-vitro functioning antibodies, 2023.
- Jo Erika Narciso, Iris Uy, April Cabang, Jenina Chavez, Juan Pablo, Gisela Padilla-Concepcion, and Eduardo Padlan. Analysis of the antibody structure based on high-resolution crystallographic studies. *New biotechnology*, 28:435–47, 04 2011. doi: 10.1016/j.nbt.2011.03.012.

- Benjamin North, Andreas Lehmann, and Roland L. Dunbrack. A new clustering of antibody cdr loop conformations. *Journal of Molecular Biology*, 406(2):228–256, 2011. ISSN 0022-2836. doi: <https://doi.org/10.1016/j.jmb.2010.10.030>. URL <https://www.sciencedirect.com/science/article/pii/S0022283610011496>.
- Tobias H. Olsen, Fergus Boyles, and Charlotte M. Deane. Observed antibody space: A diverse database of cleaned, annotated, and translated unpaired and paired antibody sequences. *Protein Science*, 31(1):141–146, 2022. doi: <https://doi.org/10.1002/pro.4205>. URL <https://onlinelibrary.wiley.com/doi/abs/10.1002/pro.4205>.
- Koichiro Saka, Taro Kakuzaki, Shoichi Metsugi, Daiki Kashiwagi, Kenji Yoshida, Manabu Wada, Hiroyuki Tsunoda, and Reiji Teramoto. Antibody design using lstm based deep generative model from phage display library for affinity maturation. *Scientific Reports*, 11(1):5852, 2021. doi: [10.1038/s41598-021-85274-7](https://doi.org/10.1038/s41598-021-85274-7). URL <https://doi.org/10.1038/s41598-021-85274-7>.
- Amir Shanehsazzadeh, Julian Alverio, George Kasun, Simon Levine, Jibrán A. Khan, Chelsea Chung, Nicolas Diaz, Breanna K. Luton, Ysis Tarter, Cailen McCloskey, Katherine B. Bateman, Hayley Carter, Dalton Chapman, Rebecca Consbruck, Alec Jaeger, Christa Kohnert, Gaelin Kopeck-Belliveau, John M. Sutton, Zheyuan Guo, Gustavo Canales, Kai Ejan, Emily Marsh, Alyssa Ruelos, Rylee Ripley, Brooke Stoddard, Rodante Caguiat, Kyra Chapman, Matthew Saunders, Jared Sharp, Douglas Ganini da Silva, Audree Feltner, Jake Ripley, Megan E. Bryant, Danni Castillo, Joshua Meier, Christian M. Stegmann, Katherine Moran, Christine Lemke, Shaheed Abdulhaqq, Lillian R. Klug, Sharrol Bachas, and Absci Corporation. In vitro validated antibody design against multiple therapeutic antigens using generative inverse folding. *bioRxiv*, 2023. doi: [10.1101/2023.12.08.570889](https://doi.org/10.1101/2023.12.08.570889). URL <https://www.biorxiv.org/content/early/2023/12/09/2023.12.08.570889>.
- Jascha Sohl-Dickstein, Eric Weiss, Niru Maheswaranathan, and Surya Ganguli. Deep unsupervised learning using nonequilibrium thermodynamics. In Francis Bach and David Blei, editors, *Proceedings of the 32nd International Conference on Machine Learning*, volume 37 of *Proceedings of Machine Learning Research*, pages 2256–2265, Lille, France, 07–09 Jul 2015. PMLR. URL <https://proceedings.mlr.press/v37/sohl-dickstein15.html>.
- Yang Song, Jascha Sohl-Dickstein, Diederik P. Kingma, Abhishek Kumar, Stefano Ermon, and Ben Poole. Score-based generative modeling through stochastic differential equations, 2021.
- Brian L. Trippe, Jason Yim, Doug Tischer, David Baker, Tamara Broderick, Regina Barzilay, and Tommi S. Jaakkola. Diffusion probabilistic modeling of protein backbones in 3d for the motif-scaffolding problem. In *The Eleventh International Conference on Learning Representations*, 2023. URL <https://openreview.net/forum?id=6TxBxqNME1Y>.
- Yuko Tsuchiya and Kenji Mizuguchi. The diversity of h3 loops determines the antigen-binding tendencies of antibody cdr loops. *Protein science : a publication of the Protein Society*, 25, 01 2016. doi: [10.1002/pro.2874](https://doi.org/10.1002/pro.2874).
- Ashish Vaswani, Noam Shazeer, Niki Parmar, Jakob Uszkoreit, Llion Jones, Aidan N. Gomez, Lukasz Kaiser, and Illia Polosukhin. Attention is all you need, 2017.
- Joseph L. Watson, David Juergens, Nathaniel R. Bennett, Brian L. Trippe, Jason Yim, Helen E. Eisenach, Woody Ahern, Andrew J. Borst, Robert J. Ragothe, Lukas F. Milles, Basile I. M. Wicky, Nikita Hanikel, Samuel J. Pellock, Alexis Courbet, William Sheffler, Jue Wang, Preetham Venkatesh, Isaac Sappington, Susana Vázquez Torres, Anna Lauko, Valentin De Bortoli, Emile Mathieu, Regina Barzilay, Tommi S. Jaakkola, Frank DiMaio, Minkyung Baek, and David Baker. Broadly applicable and accurate protein design by integrating structure prediction networks and diffusion generative models. *bioRxiv*, 2022. doi: [10.1101/2022.12.09.519842](https://doi.org/10.1101/2022.12.09.519842). URL <https://www.biorxiv.org/content/early/2022/12/10/2022.12.09.519842>.
- Zachary Wu, Kadina E. Johnston, Frances H. Arnold, and Kevin K. Yang. Protein sequence design with deep generative models. *Current Opinion in Chemical Biology*, 65:18–27, 2021. ISSN 1367-5931. doi: <https://doi.org/10.1016/j.cbpa.2021.04.004>. URL <https://www.sciencedirect.com/science/article/pii/S136759312100051X>. Mechanistic Biology * Machine Learning in Chemical Biology.

- Jason Yim, Brian L Trippe, Valentin De Bortoli, Emile Mathieu, Arnaud Doucet, Regina Barzilay, and Tommi Jaakkola. Se(3) diffusion model with application to protein backbone generation. *arXiv preprint arXiv:2302.02277*, 2023.
- Yangtian Zhan, Zuobai Zhang, Bozitao Zhong, Sanchit Misra, and Jian Tang. Diffpack: A torsional diffusion model for autoregressive protein side-chain packing, 2023.
- Cheng Zhang, Adam Leach, Thomas Makkink, Miguel Arbesú, Ibtissem Kadri, Daniel Luo, Liron Mizrahi, Sabine Krichen, Maren Lang, Andrey Tovchigrechko, Nicolas Lopez Carranza, Uğur Şahin, Karim Beguir, Michael Rooney, and Yunguan Fu. Framedipt: Se(3) diffusion model for protein structure inpainting. *bioRxiv*, 2023. doi: 10.1101/2023.11.21.568057. URL <https://www.biorxiv.org/content/early/2023/11/21/2023.11.21.568057>.
- Yang Zhang and Jeffrey Skolnick. Scoring function for automated assessment of protein structure template quality. *Proteins*, 57(4):702—710, December 2004. ISSN 0887-3585. doi: 10.1002/prot.20264. URL <https://doi.org/10.1002/prot.20264>.